Ultrafast trapping times in ion implanted InP

C. Carmody,[a)] H. Boudinov,[b)] H. H. Tan, and C. Jagadish
*Department of Electronic Materials Engineering, Research School of Physical Sciences and Engineering,
The Australian National University, Canberra, ACT 0200, Australia*

M. J. Lederer, V. Kolev, and B. Luther-Davies
*Laser Physics Centre, Research School of Physical Sciences and Engineering, The Australian National
University, Canberra, ACT 0200, Australia*

L. V. Dao and M. Gal
School of Physics, University of New South Wales, Sydney, NSW, 2052, Australia

As^+ and P^+ implantation was performed on semi-insulating (SI) and p-type InP samples for the purpose of creating a material suitable for ultrafast optoelectronic applications. SI InP samples were implanted with a dose of 1×10^{16} cm^{-2} and p-type InP was implanted with doses between 1×10^{12} and 1×10^{16} cm^{-2}. Subsequently, rapid thermal annealing at temperatures between 400 and 700 °C was performed for 30 sec. Hall-effect measurements, double-crystal x-ray diffraction, and time-resolved femtosecond differential reflectivity showed that, for the highest-annealing temperatures, the implanted SI InP samples exhibited high mobility, low resistivity, short response times, and minimal structural damage. Similar measurements on implanted p-type InP showed that the fast response time, high mobility, and good structural recovery could be retained while increasing the resistivity. © *2002 American Institute of Physics.* [DOI: 10.1063/1.1493651]

I. INTRODUCTION

The discovery of ultrafast carrier recombination characteristics in GaAs grown by molecular-beam epitaxy at low-substrate temperatures (LT-GaAs)[1–3] has led to continued research into semiconductor materials for subpicosecond optoelectronic applications. This is due to the fact that LT-GaAs has such superior characteristics as short carrier lifetime, high resistivity ($>10^5$ Ω cm), and high-electron mobility. It has been shown recently that ion implantation of GaAs can result in a material with properties similar to those of LT-GaAs.[4–6] Broad studies made on LT-GaAs have led to the conclusion that non-stoichiometry of this material with a high-arsenic excess in the form of antisite defects and As precipitates is the main reason for high resistivity and fast recombination of photocarriers.[7]

These results have stimulated efforts to understand electrical and structural properties of LT indium phosphide.[8] It was found that the LT-InP epilayers were highly conductive and that the dominant intrinsic deep level defect was present in concentrations as high as 10^{19} cm^{-3}.[8] The mechanism responsible for the n-type conductivity has been attributed to an abundant presence of P_{In} antisites, introduced during off-stoichiometric InP growth at low temperature.

The antisite defects in III–V materials have been intensively studied, and particularly in GaAs, the arsenic antisite is responsible for the semi-insulating behavior.[9] In InP, the presence of these defects has a different character, creating n-type free carriers.[8]

In this article, we have investigated the possibility to achieve high resistivity and ultrashort photoexcited carrier lifetimes in As^+- and P^+-implanted InP.

II. EXPERIMENT

Semi-insulating Fe-doped InP samples were implanted with As^+ and P^+ ions at energies of 2 and 1 MeV, respectively, at a dose of 1×10^{16} cm^{-2}, and at a substrate temperature of 200 °C. Therefore, damage profiles for both types of implanted species placed the maximum damage at a depth of approximately 1 μm from the surface. The amount of damage is expected to be higher for the As^+-implanted sample due to the heavier ion mass. P-type epilayers with two different carrier concentrations ($\sim$3.4e17 and $\sim$1.3e18 cm^{-3}) were grown to a thickness of $\sim$1.5 μm on semi-insulating InP substrates by metal-organic chemical-vapor deposition, and then implanted under the same conditions to doses between 1×10^{12} and 1×10^{16} cm^{-2}. Subsequently, samples were annealed by rapid thermal annealing (RTA) at 400, 500, 600, and 700 °C for 30 s in an Ar atmosphere. Time-resolved femtosecond differential reflectivity of the surface was measured using a standard wavelength-degenerate pump-probe setup. 75 MHz, 100 fs pulses from a mode-locked Ti:Sapphire laser were tuned to a wavelength of 895 nm, exciting the samples with pump fluences (F_{pump}) of 50 or 5 μJ cm^{-2}. Time-resolved photoluminescence (TRPL) was measured using a femtosecond self-mode locked Ti:sapphire laser. The laser was tunable between 750 and 900 nm, the pulse width was 80 fs, the repetition rate 85 MHz, and the output power was 200 mW at λ=780 nm. Double-crystal x-ray diffraction (DCXRD) and Hall-effect measurements (Van der Pauw method[10]) were also performed on these samples.

[a)]Electronic mail: cyc109@rsphysse.anu.edu.au
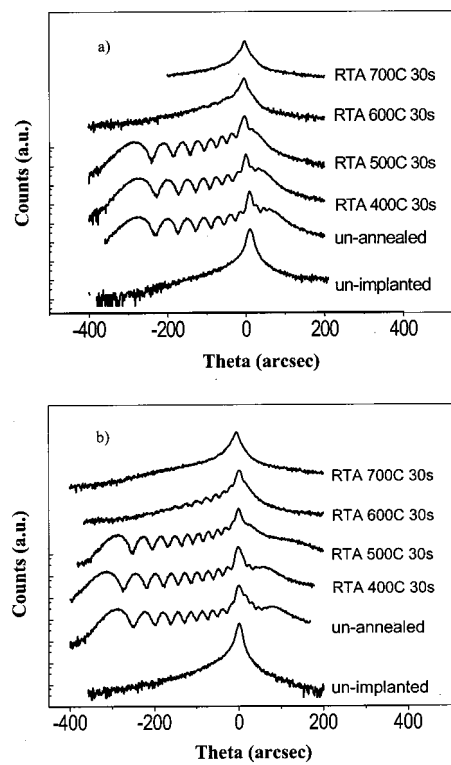[b)]Permanent address: Instituto de Fisica, UFRGS, Porto Alegre, Brazil.

FIG. 1. X-ray rocking curves from InP implanted at 200 °C with a dose of 1×10^{16} cm^{-2}. 1 MeV P$^+$ (a) and 2 MeV As$^+$ (b). Spectra vertically shifted for clarity.
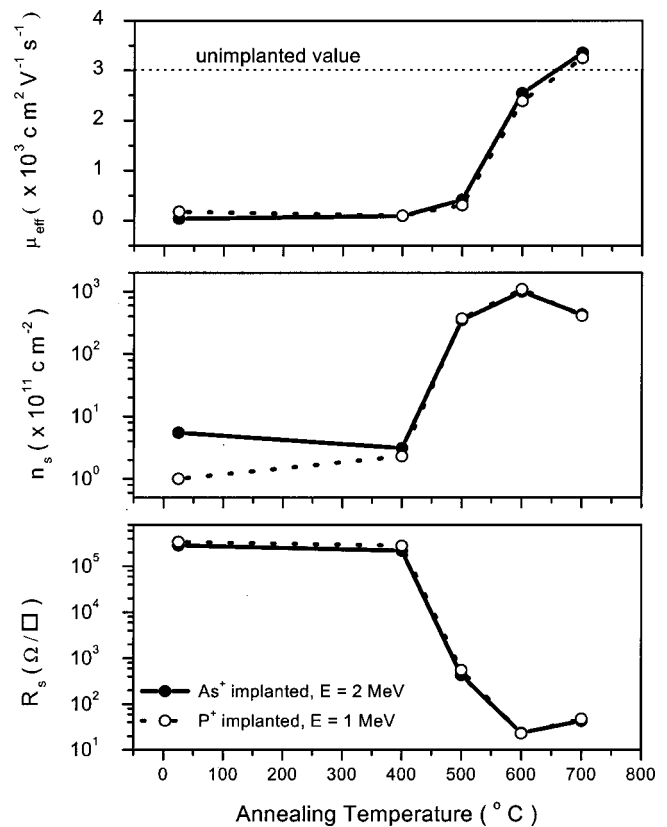

FIG. 2. Mobility (a), sheet carrier concentration (b), and sheet resistance (c) as a function of annealing temperature, for InP implanted with P$^+$ and As$^+$ to a dose of 1×10^{16} cm^{-2}.

III. RESULTS AND DISCUSSION

Figure 1 shows the DCXRD spectra from *s-i* InP samples implanted with As$^+$ and P$^+$ to a dose of 1 $\times 10^{16}$ cm^{-2}. The spectra are markedly different to those obtained by As$^+$ ion implantation into GaAs for the same dose:[11] for those samples which were unannealed or annealed at or below 500 °C, there are periodic fringes on the negative angle side of the rocking curves. These fringes have been associated with a region of positive strain (expansion) created by implantation. Additional features can also be seen on the positive angle side of the main peak, which are probably related to vacancies caused by the implantation. A slightly smaller periodicity is observed in the negative-angle fringes for the As$^+$-implanted samples, evidence of a thicker region of damage in comparison to the P$^+$-implanted samples. An annealing temperature of 600 °C is sufficient to relieve most of the expansive strain in both sets of samples. After annealing at 700 °C, the DCXRD spectra appear similar to those of the unimplanted samples. The broader full width at half maximum of the main peak is indicative of residual defects in the material.

Figure 2 shows evolution of the mobility μ_{eff}, the sheet carrier concentration n_s, and the sheet resistance R_s, with varying annealing temperature, determined from Hall-effect measurements. The corresponding values in an unimplanted semi-insulating InP wafer are approximately 2000 cm^2 V^{-1} s^{-1}, 10^7 cm^{-2}, and 3×10^8 Ω/□, respectively. The electrical properties of the samples are similar, irrespective of whether they were implanted with As$^+$ or P$^+$. After implantation, the

mobility drops to 180 cm^2 V^{-1} s^{-1} for the P$^+$-implanted sample and 40 cm^2 V^{-1} s^{-1} for the As$^+$-implanted sample; n_s increases to $\sim 10^{11}$ cm^{-2} and R_s drops to $\sim 10^5$ Ω/□ for both As$^+$- and P$^+$-implanted samples. The electrical properties of the "as-implanted" sample, consistent with a material that contains a large number of defects, are not changed significantly by annealing at temperatures below 500 °C. After annealing at 600 °C, the effective mobility has increased to the unimplanted value of ~ 2000 cm^2 V^{-1} s^{-1}, the sheet carrier concentration has peaked at $\sim 10^{14}$ cm^{-2}, and the sheet resistance has dropped to a minimum of ~ 20 Ω/□. Annealing at 700 °C causes the mobility to rise ~ 1.5 times above the unimplanted value to ~ 3000 cm^2 V^{-1} s^{-1}. For annealing temperatures above 500 °C, n_s becomes very large and the sheet resistance decreases accordingly, indicating the presence of shallow donorlike levels.

Disruption of the Fe doping sites, whose role in the substrate is to compensate for inevitable shallow donor formation during crystal growth, may have allowed the donors to reactivate and contribute to the large sheet carrier concentration. The presence of this effect is also indicated by the very high-mobility values for annealing at 700 °C. However, the typical Fe doping concentration is 1×10^{16} cm^{-3}, resulting in a sheet concentration of 1×10^{12} cm^{-2} in a 1-μm-thick layer of InP. Thus, even if all the Fe acceptors were deactivated, the maximum increase in n_s that could be achieved by this mechanism is of the order of 1×10^{12} cm^{-2}. It can be seen that at annealing temperatures greater than 500 °C, n_s is
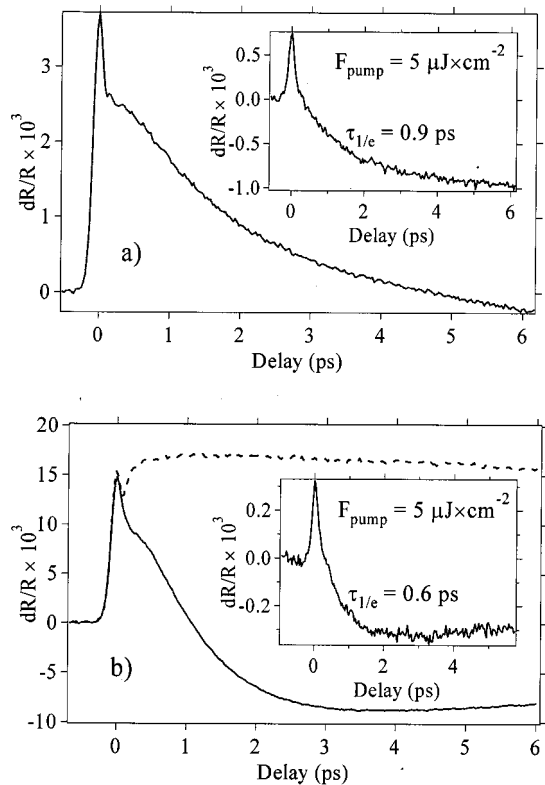
FIG. 3. dR/R signals of P^+ implanted (a), and As^+ implanted (b) samples annealed at 700 °C (unimplanted trace shown by dotted line). $F_{pump} = 50$ μJ$\times$cm^{-2} corresponding to an injection density of $\sim 2 \times 10^{18}$ cm^{-3}. Insets show traces for $F_{pump} = 5$ μJ$\times$cm^{-2}.

FIG. 4. Mobility (a), sheet carrier concentration (b), and sheet resistance (c) as a function of P^+ implant dose, for p-type InP with hole concentrations $\sim 3.4 \times 10^{17}$ and $\sim 1.3 \times 10^{18}$ cm^{-3}. Samples annealed at 600 °C for 30 s. Open symbols signify p type, and closed symbols signify n type. Joining lines are guides for the eye only.

in excess of 10^{13} cm^{-2}. Additionally, the similarity of the Hall-effect data from As^+- or P^+-implanted samples suggests that the implantation species is not responsible for the annealing-induced changes. Hence, the conclusion that these shallow donorlike levels are created by defects in the crystal structure itself, as a result of the implantation and annealing process.[12,13]

Figure 3 presents the time evolution of normalized differential surface reflectivity (dR/R). Typically, these differential signals originate in the refractive index change Δn, induced by the optically generated carriers. Since the measurement wavelength ($\lambda = 895$ nm) is shorter than the band-gap wavelength ($\lambda_{BG} = 917$ nm), Δn and dR/R are both positive. Comparing the signal from the unimplanted sample [dashed curve in Fig. 3(b)] with those from implanted samples illustrates the drastic change induced by ion implantation and annealing. The initial peak in all cases corresponds to the pump-probe correlation, after which carriers thermalize, undergo cooling and trapping, and for long delay times (tens of ps-not shown), undergo recombination processes.[14,15] In the data, taken with a pump fluence of 50 μJ$\times$cm^{-2}, there is a slight "shoulder" visible following the pump-probe correlation peak. This may be attributed to hot carrier dynamics, induced by two-photon absorption at high-pump fluences (compare insets for low-fluence excitation). Figure 3 clearly shows that even at high-annealing temperatures traps still exist, in agreement with the DCXRD results.
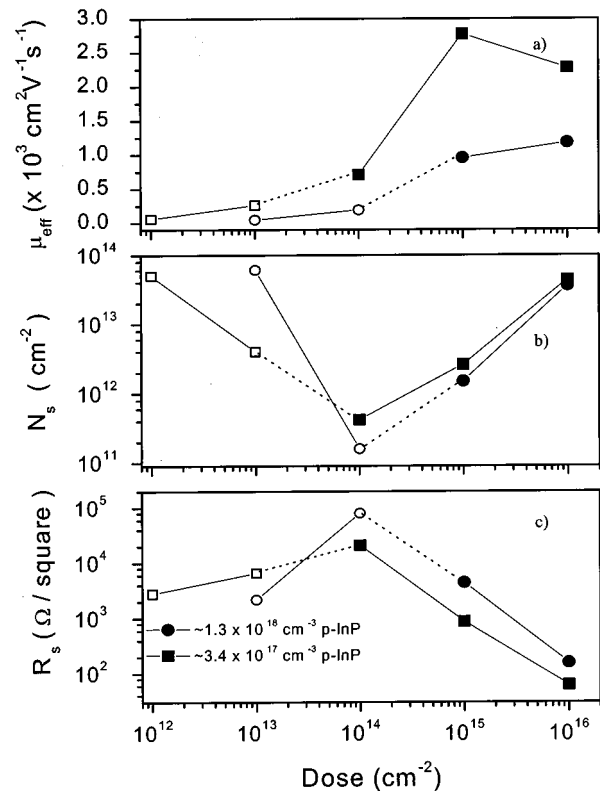
The data for low-pump fluence (5 μJ$\times$cm^{-2}) were normalized after the background values were subtracted, and the delays at which the dR/R value fell to $1/e$ were taken as characteristic trapping related response times. These were 0.9 ps in the P^+-implanted case and 0.6 ps in the As^+-implanted case.

The results thus far have indicated that it is possible to create a good quality material with a fast response time and good mobility by implanting semi-insulating InP and annealing at high temperatures, but at the expense of low-sheet resistance. Low-sheet resistance is associated with high-dark currents in photodetectors and is therefore considered undesirable. However, such materials may still find application as saturable absorbers for the mode locking of solid-state lasers. Continuing with the main aim of producing fast photodetectors, p-type epilayers were used for a round of similar experiments, to see if the donors produced by implantation could be compensated for.

Figure 4 shows the Hall-effect results for P^+ implantation into two different p-type InP samples at doses between 1×10^{12} and 1×10^{16} cm^{-2}, and subsequently annealed at 600 °C. Within this range, a critical dose exists at which implantation compensates the p-type material. For an acceptor concentration of $\sim 3.4 \times 10^{17}$ cm^{-3}, an implant dose between 10^{13} and 10^{14} cm^{-2} is required. For an acceptor concentration of $\sim 1.3 \times 10^{18}$ cm^{-3}, an implant dose between 10^{14} and 10^{15} cm^{-2} is required. Further experiments within this critical range could pinpoint the exact dose for transition
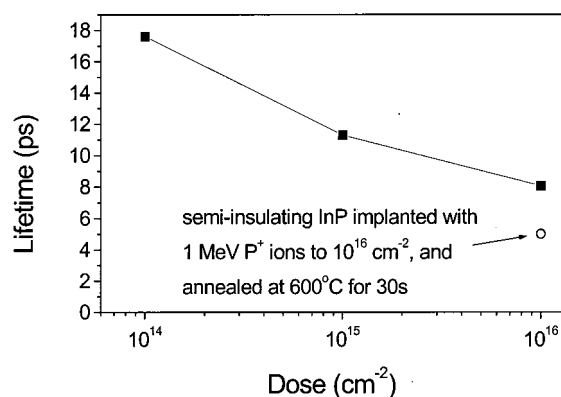
J. Appl. Phys., Vol. 92, No. 5, 1 September 2002

Carmody *et al.*   2423

FIG. 5. Plot of time-resolved photoluminescence decay times for *p*-InP ($\sim 3.4 \times 10^{17}$ cm^{-3}) implanted with different doses of 1 MeV P$^+$ ions at 200 °C, subsequently annealed by RTA 600 °C 30 s.

and subsequent annealing at temperatures between 400 and 700 °C were investigated using DCXRD, Hall-effect measurements, time-resolved femtosecond differential reflectivity, and photoluminescence. Annealing at high temperatures (700 °C) is required to remove strain and reduce defects introduced during implantation. This also results in a material with high mobility, high-sheet carrier concentration, low resistivity, and short (picosecond) carrier lifetime. As$^+$ implantation results in a slightly faster material than P$^+$ implantation. By choosing the appropriate implant dose, *p*-type hole concentration, and annealing temperature, *p*-type InP implanted with P$^+$ ions could be used for the fabrication of ultrafast photodetectors. For *p*-type InP with a hole concentration of $\sim 10^{17}$ cm^{-3} the critical implant dose lies between 10^{13} and 10^{14} cm^{-2}, and for a hole concentration of $\sim 10^{18}$ cm^{-3}, the critical dose is between 10^{14} and 10^{15} cm^{-2}, for the samples annealed at 600 °C.

from *p*- to *n*-type. This transition dose will also produce the highest-sheet resistance values for implanted *p*-type InP.

Finally, in order to obtain characteristic times for the removal of carriers from the conduction and valence bands (important for ultrafast photodetector applications) we have studied the time-resolved photoluminescence (TRPL) of some samples. Figure 5 shows the TRPL decay time of P$^+$-implanted *p*-type InP ($\sim 3.4 \times 10^{17}$ cm^{-3}) for different ion doses after annealing at 600 °C. The decay times for implanted semi-insulating and *p*-type InP are of a similar magnitude (see Fig. 5). As the ion dose is increased, the carrier lifetime decreases. An implant dose of 1 $\times 10^{14}$ cm^{-2}, which will compensate the material, results in a photoluminescence decay time of 18 ps. The decay time of unimplanted, SI-InP is of the order of a nanosecond, thus implantation results in a several orders of magnitude shortening of the decay time. Defects induced by implantation are known to dramatically increase the trapping efficiency of the material.[6] Thus, by implanting *p*–InP, it is possible to produce a material with properties suitable for fast photodetectors.

IV. CONCLUSION

The electrical, optical and structural changes to semi-insulating InP as a result of implantation with As$^+$ and P$^+$

[1] F. W. Smith, A. R. Calawa, C.-L. Chen, M. J. Manfra, and L. J. Mahooney, IEEE Electron Device Lett. **9**, 77 (1988).
[2] S. Gupta and J. F. Whitaker, IEEE J. Quantum Electron. **28**, 2464 (1992).
[3] M. Kaminska and E. R. Weber, Mater. Sci. Forum **83–87**, 1033 (1992).
[4] A. Claverie, F. Namavar, and Z. Lilienthal-Weber, Appl. Phys. Lett. **62**, 1271 (1993).
[5] A. Krotkus, S. Marcinkevicius, J. Jasinski, M. Kaminska, H. H. Tan, and C. Jagadish, Appl. Phys. Lett. **66**, 3304 (1995).
[6] C. Jagadish, H. H. Tan, A. Krotkus, S. Marcinkevicius, K. P. Korona, and M. Kaminska, Appl. Phys. Lett. **68**, 2225 (1996).
[7] D. C. Look, Thin Solid Films **231**, 61 (1993).
[8] B. W. Liang, P. Z. Lee, D. W. Shih, and C. W. Tu, Appl. Phys. Lett. **60**, 2104 (1992).
[9] W. M. Chen, P. Dreszer, A. Prasad, A. Kurpiewski, W. Walukiewicz, E. R. Weber, E. Sörman, B. Monemar, B. W. Liang, and C. W. Tu, J. Appl. Phys. **76**, 600 (1994).
[10] L. J. Van der Pauw, Philips Res. Rep. **13**, 1 (1958).
[11] H. H. Tan, C. Jagadish, K. P. Korona, J. Jasinski, M. Kaminska, R. Viselga, S. Marcinkevicius, and A. Krotkus, IEEE J. Sel. Top. Quantum Electron. **2**, 636 (1996).
[12] S. Radautsan, I. Tiginyanu, and N. Pyshnaya, Phys. Status Solidi A **108**, K59 (1988).
[13] K. Kuriyama, S. Satoh, K. Sakai, and K. Yokoyama, Nucl. Instrum. Methods Phys. Res. B **127/128**, 456 (1997).
[14] F. Ganikhanov, G.-R. Lin, W.-C. Chen, C.-S. Chang, and C.-L. Pan, Appl. Phys. Lett. **67**, 3465 (1995).
[15] J. Shah, *Ultrafast Spectroscopy of Semiconductors and Semiconductor Nanostructures* (Springer, Heidelberg, Germany, 1996).